Electronic Supplementary Material (ESI) for Soft Matter.

Supplementary Information

Title: Self-assembly of 33-mer gliadin peptide oligomers

Authors: M. G. Herrera[1], L. A. Benedini [1], C. Lonez [2], P.L. Schilardi [3], T. Hellweg [4], J-M Ruysschaert [5] and V. I. Dodero [1,6]*

Affiliation: [1] Departamento de Química-INQUISUR, Universidad Nacional del Su-CONICET, Av. Alem 1253, Bahía Blanca, Argentina. [2]Department of Veterinary Medicine, University of Cambridge, United Kingdom. [3] Instituto de Investigaciones Fisicoquímicas Teóricas y Aplicadas (INIFTA), CONICET – Departamento de Química, Facultad de Ciencias Exactas, UNLP, CC16, Suc. 4(1900) La Plata, Buenos Aires, Argentina.[4] Universität Bielefeld, Fakultät für Chemie, Physikalische und Biophysikalische Chemie, Universitätsstr. 25, 33615 Bielefeld, Germany, [5] Structure and Function of Biological Membranes, Université Libre de Bruxelles, Belgium, [6] Universität Bielefeld, Fakultät für Chemie, Organische Chemie, Universitätsstr. 25, 33615 Bielefeld, Germany.

*To whom correspondence should be addressed.

1. UV-Visible

UV-Visible spectroscopy was used to evaluate the self-assembly of 33-mer gliadin peptide. The change in the position of the maximum absorbance peak of Tyrosine was studied by second derivative procedure using the third order Savitzky-Golay polynomial smoothing. We observed a change of the peak position from 274.5 nm to 275.0 nm when the concentration was increased from ≈ 60 μM to 80 μM. A similar behavior was observed from ≈ 150 μM to ≈ 200 μM and the maximum shifted from 275.0 nm to 275.5 nm. These changes indicate that Tyrosine is less exposed to the solvent due to the formation of self-assembled structures.

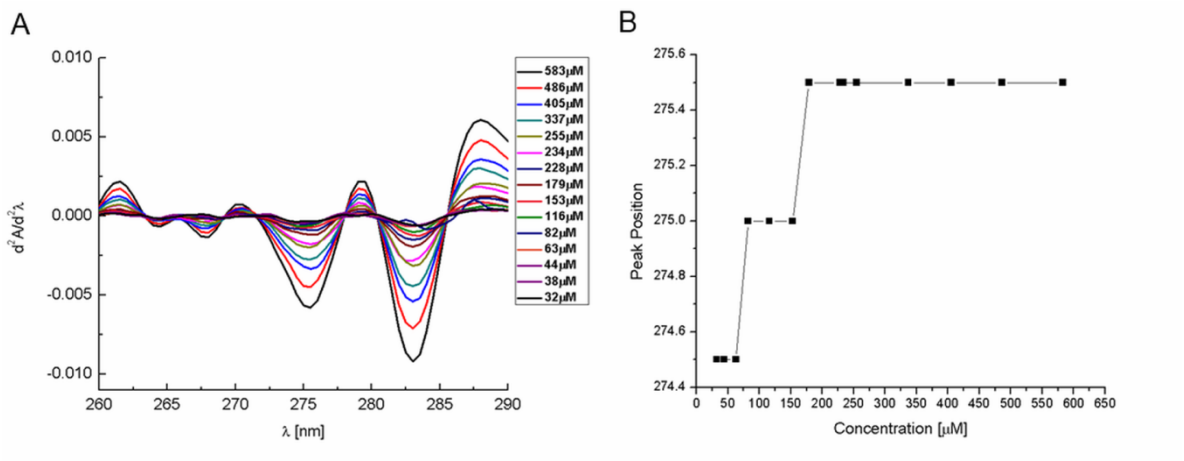

Figure S1. A) UV-Visible secondary derivative spectra of 33-mer peptide solutions in water at different concentrations. B) Peak position is concentration dependent..

2. DLS Theory and Data Analysis:

Due to fluctuations caused by the Brownian motion of the scattering particles, the scattering intensity is a fluctuating parameter. These fluctuations of *I* can be analyzed using correlation functions[1]. The normalized electrical field autocorrelation function g_1 contains information about the dynamics of the scattering system, in this case of the 33 mer solution:

$$g1\ (\tau) = \frac{< Es*(t)\ Es\ (t+\tau) >}{< I >} \qquad (1)$$

With E_s= scattered electrical field, E_s* = complex conjugate of E_s and *t* =time.

In the case of a mono-disperse ideal sample $g1\ (\tau)$ it is represented by a single exponential:

$$g1\ (\tau) = exp\ (-\Gamma\tau) \qquad (2)$$

with $\Gamma = D\ q^2$, with D as a translational diffusion coefficient and q the scattering vector [1] Normally samples are poly-disperse and the decay of the correlation function must be described by a weighted sum of exponentials:

$$g1\ (\tau) = \int_0^{+\infty} G(\Gamma)\exp\ (\ -\ \Gamma\tau)\ d\Gamma \qquad (3)$$

$G(\Gamma)$ is the distribution function of the relaxation rates. The analysis of the function given by Eq. (3) can be performed with different methods. The most frequently applied are the method of cumulants [2, 3] and the analysis of Eq. (3), by an inverse Laplace transformation by using for example of the FORTRAN program CONTIN. [4, 5] Multi-modal correlation functions can also be fitted with sums of exponentials using non-linear least-square methods. [6] From the mean value of the relaxation rate Γ (z-average) one can obtain $\overline{D}$:

$$\overline{D} = \overline{\Gamma} q^2 \quad (4)$$

$\overline{D}$ is the mean translational diffusion coefficient.The scattering vector q is given by:

$$q = \frac{4\pi n}{\lambda} sin\left(\frac{\theta}{2}\right) \qquad (5)$$

Here λ is the wavelength of the incident laser-beam, n the refractive index of the scattering medium and θ scattering angle. Knowing the value for D the Stokes radius R_s can be calculated from the Stokes-Einstein equation.

$$Rs = kB\frac{T}{6\pi\eta D} \qquad \text{(Eq. 6)}$$

The diffusion coefficients may show concentration dependence, indicating inter-particle interactions. For the translational diffusion coefficient of interacting particles in dilute solution a linear dependence on the volume fraction Φ is expected. [7]

$$D_o = D\,[1+ \alpha\Phi] \qquad (7)$$

Here, α is the dynamic virial coefficient and D_o the self-diffusion coefficient. From Eq. (7), the self-diffusion coefficient can be obtained by extrapolation to zero volume fraction (~concentration).

Based on the theory described in this section, the mean R_h values obtained for each group of size particles were calculated in the present work.

3. Atomic force Microscopy

1. Radius, volume and number of molecules calculations.

The volume, the radius and the molecular mass of a protein could be obtained with a good estimation by AFM. [8,9,10]

In this article we calculated the radius of the isolated 33-mer spherical oligomers observed at 6 μM. Taking into account that AFM images are obtained by surface interaction and that the tip used, introduce a distortion, direct estimation of the oligomers radius is not possible. However, the volume of the spheres might be determined as it was proposed by Pietrasanta et.al. in equation 1 (Eq.7) [11].

$$Vs = \pi(\mathrm{h}/6)\left[3r^2 + \mathrm{h}^2\right] \qquad (7)$$

In which (h) is the average height of the spheres, and (r) is the radius estimated as the half of the full width at the half maximum height (FWHM). This last consideration is necessary to compensate the errors introduced by the conical shape of the tip, avoiding an

overestimation of the protein width. [12] For these calculations, an average of 50 spheres were used in each sample.

Then, the radius was calculated using the equation of the volume of the sphere (Eq.8).

$$Vs = \frac{4}{3}\pi r^3 \quad (8)$$

In addition, the average volume obtained was used to calculate the number of molecules that possibly composed the oligomers. For this, the mass of the oligomer is calculated employing the equation proposed by Tanford (Eq. 9). [13]

$$V = \frac{M}{N}(V_2 + \delta V_1) \quad (9)$$

where M is the molecular mass of the oligomer, N the Avogadro Number, V_2 the partial specific volume, calculated by molecular diffusion estimations (for this an average value of 0.73cm^3/g was calculated for globular proteins), V_1 is the pure solvent volume, which is assigned a value of 1 cm^3 /g and δ is the specific solvation, calculated by isotopic exchange experiments of ovalbumin, using H_2O^{18}. This value is estimated to be equal for all the proteins.

Dividing the mass obtained for the oligomer (by Eq.9) by the molecular mass of a single molecule of peptide (3917g/mol), the average number of molecules presented in the sphere can be obtained.

2 Supplementary AFM Images

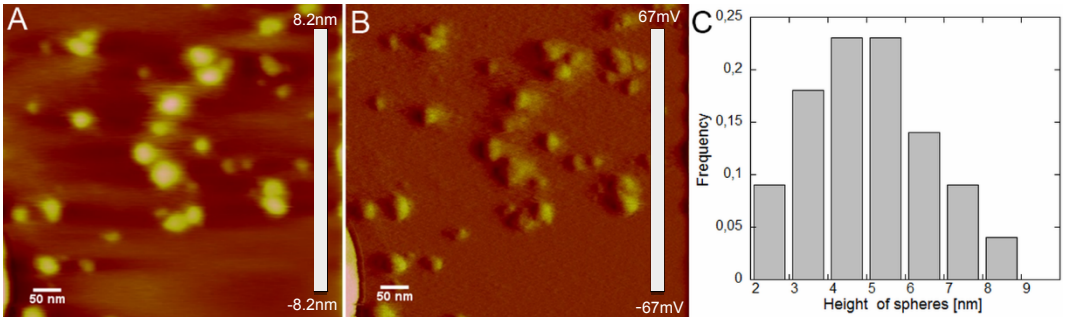

Figure S3. Selected topographic images from Figure 3 in the main text. A) Spherical oligomers, B) annular oligomers, C) planar "sheet" like structures. D), E) and F) Height distribution of images A), B) and C), respectively. For this statistical analysis, the height of 50 particles were considered.

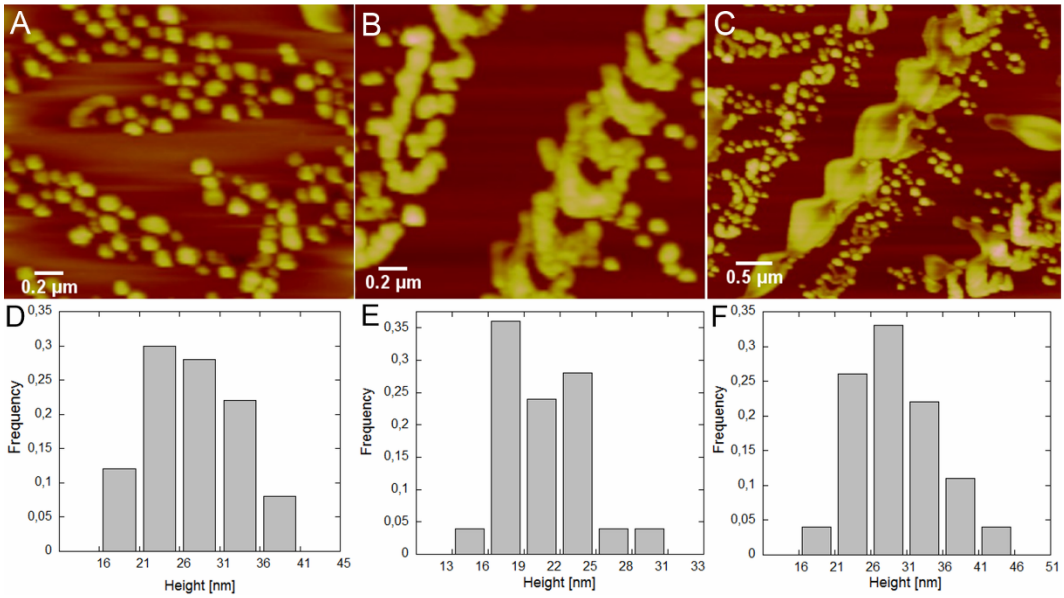

Figure S4. Selected Images of 33-mer peptide spherical oligomers observed at 610µM in water, pH7 in: A) topographic and B) deflection error image. C) Height distribution of the detected particles.

4 Fractal Dimension:

Fractal Dimension is a measure of the complexity of a system. It is a scaling rule that is used to compare how pattern details change when the scale varied from minor to major resolution. Mathematically, it is expressed as

$$N \propto \epsilon^{-Df}$$

Where D_f is the fractal dimension, N is the number of pieces observed in each new resolution and ϵ is the scale used for each pieces.

FracLac software from Image J was employed for the determination of D_f using the box counting procedure. The basic procedure is to lay systematically a series of grids of decreasing calibre (the boxes) over an image and record data (the counting) for each successive calibre. The program gives access to D_f obtained by the application of several mathematical algorithms.

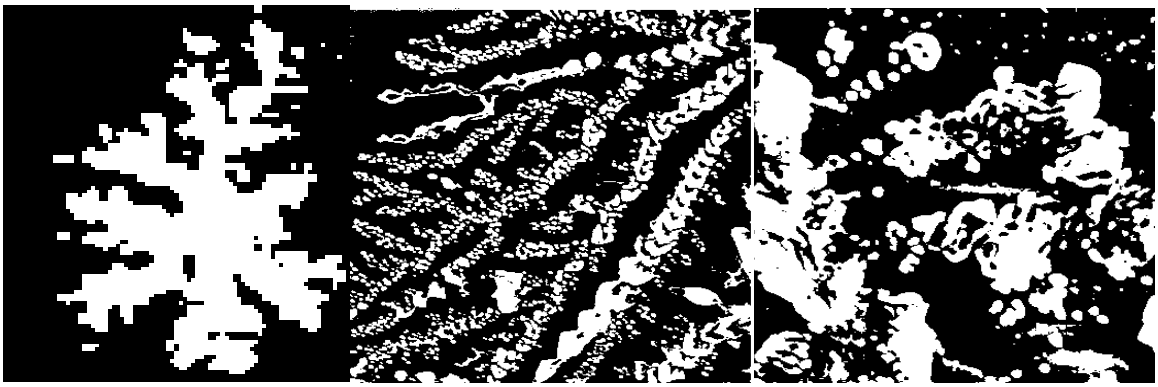

Figure S5. 8 bit images employed for D_f calculation at the selected concentration of 33-mer peptide solution: A) 6 μM, B) 60 μM, C) of 250 μM.

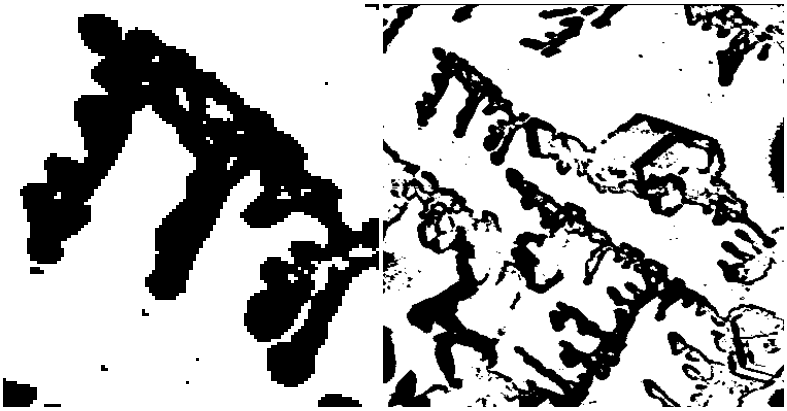

Figure S6. 8 bit images employed to calculate D_f of 33-mer peptide at 610μM deposited on bare mica.

5 Scanning Electron Microscopy (SEM)

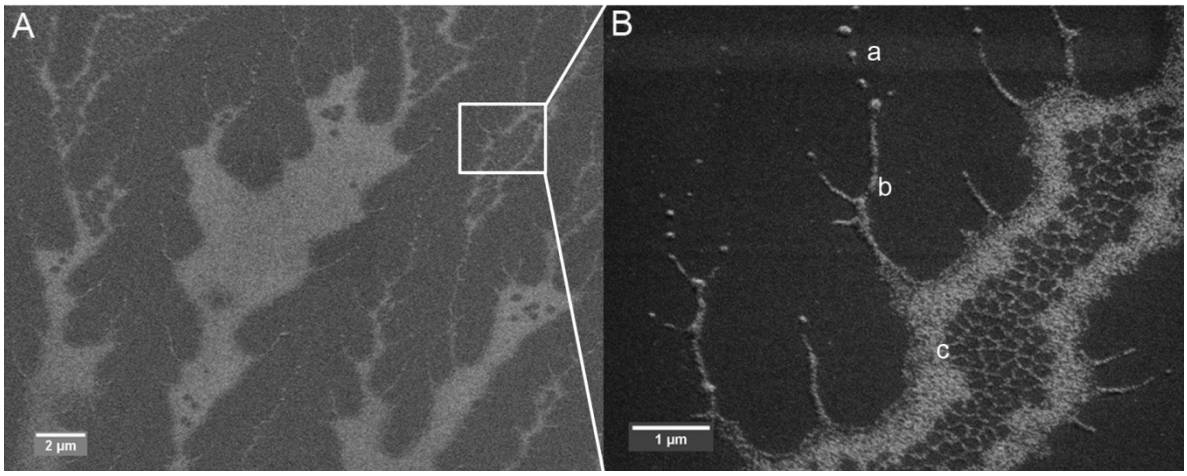

Figure S7. SEM of 33-mer peptide at 610μM in aqueous solution at pH 7.0. A) Image presenting the quaternary structures made mainly of plaques and filaments. B) Zoom of the region marked as square in image A, showing in details the micro-arrange of the peptide (a) spheres, (b) filaments and (c) plaques.

Supplementary References:

1. B. J. P. Berne, R, *Dynamic Light Scattering: With Applications to Chemistry, Biology, and Physics*, Wiley, New York, 1976.
2. D. E. Koppel, *The Journal of chemical physics*, 1972, **57**, 4814-4820.
3. C. B. Bargeron, *The Journal of chemical physics*, 1974, **61**, 2134-2138.
4. S. W. Provencher, *Computer Physics Communications*, 1982, **27**, 229-242.
5. S. W. Provencher, *Computer Physics Communications*, 1982, **27**, 213-227.
6. P. R. Bevington, *Data Reduction and Error Analysis for the Physical Sciences*, McGraw-Hill, New York 1969.
7. D. Guest and D. Langevin, *Journal of Colloid and Interface Science*, 1986, **112**, 208-220.
8. P. W. Eaton, Paul. , *Atomic Force Microscopy* Oxford University Press 2010.
9. I. Greving, M. Cai, F. Vollrath and H. C. Schniepp, *Biomacromolecules*, 2012, **13**, 676-682.
10. S. W. Schneider, J. Larmer, R. M. Henderson and H. Oberleithner, *Pflugers Archiv : European journal of physiology*, 1998, **435**, 362-367.
11. L. I. Pietrasanta, D. Thrower, W. Hsieh, S. Rao, O. Stemmann, J. Lechner, J. Carbon and H. Hansma, *Proceedings of the National Academy of Sciences of the United States of America*, 1999, **96**, 3757-3762.
12. W. Fritzsche, A. Schaper and T. M. Jovin, *Chromosoma*, 1994, **103**, 231-236.

13. C. Tanford, *Physical Chemistry of Macromolecules*, John Wiley and Sons Unites States of America, 1961.